Commun. Theor. Phys. (Beijing, China) **37** (2002) pp 759–767

Vol. 37, No. 6, June 15, 2002

Application of Local Activity Theory of Cellular Neural Network with Two Ports to the Coupled Lorenz-Cell Model*

MIN Le-Quan and YU Na

Department of Mathematics and Mechanics, University of Science and Technology, Beijing 100083, China

(Received May 30, 2001; Revised December 10, 2001)

Abstract *Some criteria for the local activity theory in two-port cellular neural network cells with three local state variables are applied to a coupled Lorenz-cell model. The numerical simulation exhibited that emergence may exist if the selected cell parameters are nearby or on the edge of chaos domain. The local activity theory has provided a new tool of studying the complexity of high dimensional coupled nonlinear physical systems.*

PACS numbers: 84.35.+i, 05.45.Jn, 02.60.cb
Key words: cellular neural network, local activity, coupled Lorenz-cell, chaos, numerical simulation

1 Introduction

Although the research on emergence and complexity has gained more and more attention during the past decade,[1−6] the determination, prediction and control of the complex patterns generated from high dimensional nonlinear systems are still far from perfect. The cellular neural network (CNN),[7] first introduced as an implementable alternative to fully-connected Hopfield neural network, has been widely studied for image processing, robotic and biological versions, and higher brain functions (see Ref. [8] and enclosed references). It is expected that some phenomena in the nature that abounds with complex patterns and structures emerging from homogeneous media operating far from thermodynamic equilibrium can be modelled and studied via the CNN.[9] The recent local activity theory,[8,9] offering a constructive analytical tool, asserts that a wide spectrum of complex behaviors may exist if the corresponding cell parameters of CNN's are chosen in or nearby the edge of chaos.[10−15] That theory has been applied to the study of the dynamics of the CNNs related to the FitzHugh–Nagumo CNN's, the Brusselator CNN's, the Gierer–Meinhart CNN's, the Oregonator CNN's, the Hodgkin–Huxley CNN's, and the biochemical model CNN's, respectively.[8−15]

The rest of this paper is organized as follows. Section 2 states the basic local activity principle set up by Chua,[8] and proposes some analytical criterion theorems for testing the local activity of the CNN's with three state variables and two ports (practically called with one viscous coupling constant and one thermal coupling constant, or called with two reaction-diffusion coefficients, etc., depending on the corresponding physical models (CNN's) described). Section 3 applies the criteria to the coupled Lorenz-cell model (CLCM) CNN's with two ports whose prototype has been studied as the coupled Lorenz-cell (or vortex-cell) models with one port (i.e., one viscous coupling constant) by Refs [17] and [18], and simulates numerically the CLCM CNN's and corresponding three-dimensional Lorenz equations. The complete proofs of our theorems (also see Ref. [15]) are stated in the Appendix.

2 Local Activity Principle and Analytical Criteria

The definition of a standard (an m-port three dimensional) CNN has been described thoroughly in Refs [8] and [9]. A two-port one-dimensional CNN with three local state variables is defined by

$$\dot{x}_i = f_1(x_i, y_i, z_i) + I_1(\boldsymbol{X})\,, \tag{1}$$

$$\dot{y}_i = f_2(x_i, y_i, z_i) + I_2(\boldsymbol{Y})\,, \tag{2}$$

$$\dot{z}_i = f_3(x_i, y_i, z_i), \quad i = 1, 2, \cdots, n\,, \tag{3}$$

where

$$\boldsymbol{X} = [x_1, x_2, \cdots, x_n]^T, \qquad \boldsymbol{Y} = [\,y_1, y_2, \cdots, y_n]^T\,,$$
$$\boldsymbol{Z} = [z_1, z_2, \cdots, z_n]^T$$

are called local state variables; I_1 and I_2 are called cell coupling terms or called two ports in terms of the network theory; the subscript i attached to x, y, and z denotes that equations (1) $\sim$ (3) represent a one-dimensional CNN.[8,9] The corresponding local state equations can be represented as[8]

$$\dot{\boldsymbol{V}}_{\boldsymbol{a}} = \boldsymbol{A}_{aa}\boldsymbol{V}_a + \boldsymbol{A}_{ab}\boldsymbol{V}_b + \boldsymbol{I}_a\,, \tag{4}$$

$$\dot{\boldsymbol{V}}_{\boldsymbol{b}} = \boldsymbol{A}_{ba}\boldsymbol{V}_a + \boldsymbol{A}_{bb}\boldsymbol{V}_b\,, \tag{5}$$

where

$$\boldsymbol{V}_a = [x, y]^T, \qquad \boldsymbol{V}_b = z, \qquad \boldsymbol{I}_a = [I_1, I_2]^T\,,$$
$$\boldsymbol{A}_{aa} = \begin{bmatrix} a_{11} & a_{12} \\ a_{21} & a_{22} \end{bmatrix}, \qquad \boldsymbol{A}_{bb} = \begin{bmatrix} a_{13} \\ a_{23} \end{bmatrix},$$
$$\boldsymbol{A}_{ba} = [a_{31}\ a_{32}], \qquad \boldsymbol{A}_{bb} = [a_{33}]\,, \tag{6}$$

*The project supported by National Natural Science Foundation of China under Grant No. 60074034 and the Foundation for University Key Teacher by the Ministry of Education of China

$$\boldsymbol{A_{aa}}(Q_i)=\begin{bmatrix}\dfrac{\partial f_1}{\partial x} & \dfrac{\partial f_1}{\partial y}\\ \dfrac{\partial f_2}{\partial x} & \dfrac{\partial f_2}{\partial y}\end{bmatrix},\qquad \boldsymbol{A_{ab}}(Q_i)=\begin{bmatrix}\dfrac{\partial f_1}{\partial z}\\ \dfrac{\partial f_2}{\partial z}\end{bmatrix},$$

$$\boldsymbol{A_{ba}}(Q_i)=\begin{bmatrix}\dfrac{\partial f_3}{\partial x}\\ \dfrac{\partial f_3}{\partial y}\end{bmatrix},\qquad \boldsymbol{A_{bb}}(Q_i)=\begin{bmatrix}\dfrac{\partial f_3}{\partial z}\end{bmatrix}, \tag{7}$$

and Q_i is an equilibrium point of Eqs (1) $\sim$ (3).

The concept of the local activity of CNN by Chua is a generalization to the concept of the activity of linear network in the network synthesis theory. For an n-port linear network $\boldsymbol{N}$, let $[\boldsymbol{V},\boldsymbol{I}]\in\boldsymbol{N}$ represent the voltage vector and the current vector, where $\boldsymbol{V}=\boldsymbol{V}(t)$ and $\boldsymbol{I}=\boldsymbol{I}(t)$ are both n-dimensional vectors.

Definition 1 $\boldsymbol{N}$ is passive if for every $[\boldsymbol{V},\boldsymbol{I}]\in\boldsymbol{N}$ and every finite t,[16]

$$\epsilon(t)=\int_{-\infty}^{t}\boldsymbol{V}(\tau)^T\boldsymbol{I}(\tau)d\tau\geq 0\,,$$

where $\boldsymbol{V}(\tau)^T$ is the transpose of $\boldsymbol{V}(\tau)$. If $\boldsymbol{N}$ is not passive, it is called active.

Remark 1 An active network has always energy to go out the network at some time.

Denote $\hat{\boldsymbol{V}}(s)$ and $\hat{\boldsymbol{I}}(s)$ as the Laplace transforms of $\boldsymbol{V}(t)$ and $\boldsymbol{I}(t)$, respectively. Assume that the relation between $\hat{\boldsymbol{V}}(s)$ and $\hat{\boldsymbol{I}}(s)$ is determined via

$$\hat{\boldsymbol{I}}(s)=Y(s)\hat{\boldsymbol{V}}(s)\,,$$

where $Y(s)$ is an $n\times n$ matrix called admittance matrix.

Chau[8] has proved that for the local state equations (4) and (5),

$$\hat{\boldsymbol{I}}_{\boldsymbol{a}}(s)=Y_Q(s)\hat{\boldsymbol{V}}_{\boldsymbol{a}}(s)\,,$$

where $Y_Q(s)$ is called CNN cell admittance and has the form,[8,9]

$$\begin{aligned}Y_Q(s)&=(s\boldsymbol{I}-\boldsymbol{A_{aa}})-\boldsymbol{A_{ab}}(s\boldsymbol{I}-\boldsymbol{A_{bb}})^{-1}\boldsymbol{A_{ba}}\\&=\begin{bmatrix}s-a_{11}-\dfrac{a_{13}a_{31}}{s-a_{33}} & -a_{12}-\dfrac{a_{13}a_{32}}{s-a_{33}}\\ -a_{21}-\dfrac{a_{23}a_{31}}{s-a_{33}} & s-a_{22}-\dfrac{a_{23}a_{32}}{s-a_{33}}\end{bmatrix}.\end{aligned} \tag{8}$$

Based on the classic positive criteria for the passive linear network,[16] Chua proposed the following local activity principle.

Lemma 1 A two-port CNN cell is locally active at a cell equilibrium point $Q\triangleq(\bar{\boldsymbol{V}}_a,\bar{\boldsymbol{V}}_b,\bar{\boldsymbol{I}}_a)$ if, and only if, its cell admittance $Y_Q(s)$ at Q satisfies at least one of the following four conditions

(i) $Y_Q(s)$ has a pole in Re $[s]>0$.

(ii) ${Y^H}_Q(\mathrm{i}\omega)={Y^\dagger}_Q(\mathrm{i}\omega)+Y_Q(\mathrm{i}\omega)$ is not a positive semi-definite matrix at some $\omega=\omega_0$, where ω_0 is any real number, and ${Y^\dagger}_Q(s)$ is constructed by taking first the transpose of $Y_Q(s)$, and then followed by the complex conjugate operation.

(iii) $Y_Q(s)$ has a simple pole $s=\mathrm{i}\omega_\rho$ on the imaginary axis, where its associated residue matrix

$$k_1\triangleq\begin{cases}\lim_{s\to\mathrm{i}\omega_\rho}(s-\mathrm{i}\omega_\rho)Y_Q(s), & \text{if}\quad \omega_\rho<\infty\,,\\ \lim_{\omega_\rho\to\infty}Y_Q(\mathrm{i}\omega_\rho)/\mathrm{i}\omega_\rho, & \text{if}\quad \omega_\rho=\infty\end{cases} \tag{9}$$

is neither a Hermitian matrix, nor a positive semi-definite Hermitian matrix.

(iv) $Y_Q(s)$ has a multiple pole on the imaginary axis.

Definition 2 Edge of chaos with respect to equilibrium point Q_i.[10,13] A "reaction-diffusion" CNN with one "diffusion coefficient" D_1 (resp. two diffusion coefficients D_1 and D_2; or three diffusion coefficients D_1, D_2, and D_3) is said to be operating on the *edge of chaos* with respect to an equilibrium point Q_i if, and only if, Q_i is both locally active and stable when $\bar{\boldsymbol{I}}_1=0$ (resp. $\bar{\boldsymbol{I}}_2=0$, and $\bar{\boldsymbol{I}}_3=0$, or $\bar{\boldsymbol{I}}_1=0$, $\bar{\boldsymbol{I}}_2=0$, and $\bar{\boldsymbol{I}}_3=0$).

Remark 2 Clearly, this definition can be extended to general CNNs with two ports (coupling terms).

From Eqs (6) $\sim$ (8) and Lemma 1, some analytical criteria for testing the local activity of the CNN's with three state variables and two ports are stated as the following theorems (also see Ref. [15]).

Theorem 1 $Y_Q(s)$ has a pole in Re $[s]>0$, if and only if, $a_{33}>0$ and $\max\{|a_{13}a_{31}|,|a_{13}a_{32}|,|a_{23}a_{31}|,|a_{23}a_{32}|\}\neq 0$.

Theorem 2 Let $b=a_{13}a_{31}a_{33}$, $c=a_{13}a_{32}a_{33}+a_{23}a_{31}a_{33}$, $d=a_{13}a_{32}-a_{23}a_{31}$, $e=a_{23}a_{32}a_{33}$, then $Y_Q(s)$ satisfies condition (ii) in Lemma 1 if, and only if at least one of the following conditions holds

1. $(a_{11}+a_{22})>0$;
2. $(a_{11}+a_{22})\leq 0, a_{33}\neq 0,\quad$ and $\quad(a_{11}+a_{22})-(a_{13}a_{31}+a_{23}a_{32})/a_{33}>0$;
3. $4a_{11}a_{22}-(a_{12}+a_{21})^2<0$;
4. $4(ba_{22}+ea_{11})-2c(a_{12}+a_{21})+d^2\neq 0$,

$$\omega^2=\frac{2a_{33}^2d^2+8be-2c^2}{4(ba_{22}+ea_{11})-2c(a_{12}+a_{21})+d^2}-a_{33}^2>0\,,$$

$$4\Big(a_{11}a_{22}-\frac{ba_{22}+ea_{11}}{a_{33}^2+\omega^2}+\frac{be}{(a_{33}^2+\omega^2)^2}\Big)-\Big(a_{12}+a_{21}-\frac{c}{a_{33}^2+\omega^2}\Big)^2-\frac{\omega^2d^2}{(a_{33}^2+\omega^2)^2}<0\,;$$

5. $a_{33}\neq 0\quad$ and $\quad 4(a_{11}a_{33}^2-b)(a_{22}a_{33}^2-e)-[(a_{12}+a_{21})a_{33}^2-c]^2<0$;

6. $a_{33} = 0$ and $4be - c^2 < 0$.

Theorem 3 $Y_Q(s)$ satisfies condition (iii) in Lemma 1 if, and only if, at least one of the following conditions holds

1. If $a_{33} = 0, \max\{|a_{13}a_{31}|,\ |a_{13}a_{32}|, |a_{23}a_{31}|, |a_{23}a_{32}|\} \neq 0$ and $a_{13}a_{32} \neq a_{23}a_{31}$;
2. If $a_{33} = 0,\ \max\{|a_{13}a_{31}|, |a_{13}a_{32}|, |a_{23}a_{31}|, |a_{23}a_{32}|\} \neq 0,\quad a_{13}a_{32} = a_{23}a_{31},$ and
   (a) $a_{13}a_{31} + a_{23}a_{32} > 0$ or
   (b) $a_{13}a_{31}a_{23}a_{32} - a_{13}^2 a_{32}^2 < 0$.

Theorem 4 $Y_Q(s)$ has not a multiple pole on the imaginary axis.

Theorems $1 \sim 4$ can be written as a computer program to test the local activity of any two-port CNN with three state variables and produce the corresponding bifurcation diagrams. As we will see in the next section, some practical physical systems can be mapped into the CNN and studied via the local activity theory.

3 CLCM CNN and Numerical Simulation

The CLCM CNN used here is taken from Jackson and Kodogeorigiou, which viscously couples N Lorenz equations,

$$\dot{x}_i = \sigma(y_i - x_i) - \mu(x_{i+1} + x_{i-1} + 2x_i)\,, \tag{10}$$

$$\dot{y}_i = -y_i - x_i z_i + r x_i - k(y_{i+1} + y_{i-1} + 2y_i)\,, \tag{11}$$

$$\dot{z}_i = x_i - b z_i, \quad (i = 1, 2, \ldots, N)\,, \tag{12}$$

where N stands for the number of vortices in the system. Let the system have periodic conditions: $x_0 = x_N$, $y_0 = y_N$, $z_0 = z_N$, $x_{N+1} = x_1$, $y_{N+1} = y_1$, $z_{N+1} = z_1$. To keep the physical meaning, it can be assumed that $\mu = -3$, and $k = 0.001$ which corresponds to the neglected thermal term $k = 0$ (see Ref. [17]). Similar to that given in Ref. [18], let $N = 32$ for numerical simulation.

In a component form, equations (10) $\sim$ (12) become

$$\dot{\boldsymbol{X}} = f_1(\boldsymbol{X}, \boldsymbol{Y}, \boldsymbol{Z}) + \mu I_1(\boldsymbol{X})\,, \tag{13}$$

$$\dot{\boldsymbol{Y}} = f_2(\boldsymbol{X}, \boldsymbol{Y}, \boldsymbol{Z}) + k I_2(\boldsymbol{Y})\,, \tag{14}$$

$$\dot{\boldsymbol{Z}} = f_3(\boldsymbol{X}, \boldsymbol{Y}, \boldsymbol{Z})\,, \tag{15}$$

where I_1 and I_2 correspond to a same $N \times N$ matrix.

The "cell equilibrium points" Q's for the restricted local activity[10] of Eqs (13) $\sim$ (15) can be determined via

$$f_1(\boldsymbol{X}, \boldsymbol{Y}, \boldsymbol{Z}) = 0, \qquad f_2(\boldsymbol{X}, \boldsymbol{Y}, \boldsymbol{Z}) = 0\,,$$
$$f_3(\boldsymbol{X}, \boldsymbol{Y}, \boldsymbol{Z}) = 0\,. \tag{16}$$

Equations (16) have a cell equilibrium point $Q_0 = (0, 0, 0)$ and two nonzero cell equilibrium points for $r > 1$,

$$Q_l = \left((-1)^l\sqrt{b(r-1)}, (-1)^l\sqrt{b(r-1)}, r - 1\right),$$
$$l = 1, 2\,. \tag{17}$$

The cell coefficients $a_{m,n}(Q_l)$s $(l = 0, 1, 2)$ are defined via the corresponding Jacobian matrix

$$\boldsymbol{A}_l \triangleq \begin{pmatrix} a_{11}(Q_l) & a_{12}(Q_l) & a_{13}(Q_l) \\ a_{21}(Q_l) & a_{22}(Q_l) & a_{23}(Q_l) \\ a_{31}(Q_l) & a_{32}(Q_l) & a_{33}(Q_l) \end{pmatrix}$$

$$\triangleq \begin{pmatrix} \dfrac{\partial f_1(\boldsymbol{U})}{\partial \boldsymbol{X}} & \dfrac{\partial f_1(\boldsymbol{U})}{\partial \boldsymbol{Y}} & \dfrac{\partial f_1(\boldsymbol{U})}{\partial \boldsymbol{Z}} \\ \dfrac{\partial f_2(\boldsymbol{U})}{\partial \boldsymbol{X}} & \dfrac{\partial f_2(\boldsymbol{U})}{\partial \boldsymbol{Y}} & \dfrac{\partial f_2(\boldsymbol{U})}{\partial \boldsymbol{Z}} \\ \dfrac{\partial f_3(\boldsymbol{U})}{\partial \boldsymbol{X}} & \dfrac{\partial f_3(\boldsymbol{U})}{\partial \boldsymbol{Y}} & \dfrac{\partial f_3(\boldsymbol{U})}{\partial \boldsymbol{Z}} \end{pmatrix}$$

$$\triangleq \begin{pmatrix} \boldsymbol{A}_{aa} & \boldsymbol{A}_{ab} \\ \boldsymbol{A}_{ba} & \boldsymbol{A}_{bb} \end{pmatrix}, \tag{18}$$

where $\boldsymbol{U} = (\boldsymbol{X}(Q_l), \boldsymbol{Y}(Q_l), \boldsymbol{Z}(Q_l))$. Consequently, the corresponding CNN cell admittance $Y_Q(s)$ can be calculated via Eqs (8) and (18).

On the other hand, one can prove that the CLCM CNN of Eqs (10) $\sim$ (12) has an origin equilibrium $P_l = (0, 0, \ldots, 0)$ and two nonzero equilibrium points for $r > 0$,

$$P_l = (x_1^l, x_2^l, \ldots, x_N^l, y_1^l, y_2^l, \ldots, y_N^l, z_1^l, z_2^l, \ldots, z_N^l)\,,$$
$$x_i^l = (-1)^{i+l-2}\sqrt{b(r-1)}\,,$$
$$y_i^l = x_i^l, \qquad z_i^l = r - 1\,,$$
$$l = 1, 2, \qquad i = 1, 2, \ldots, N\,. \tag{19}$$

Now let us rewrite the system of Eqs (10) $\sim$ (12) into a $3 \times N$ vector differential equations by choosing a row-wise order scheme,

$$x_i \longrightarrow x_i, \quad y_i \longrightarrow x_{N+i}, \quad z_i \longrightarrow x_{2N+i}\,,$$
$$i = 1, 2, \ldots, N\,. \tag{20}$$

Denote

$$\boldsymbol{X} = [x_1, x_2, \ldots, x_{3N}]\,.$$

Then the CLCM CNN of Eqs (10) $\sim$ (12) can be rewritten as

$$\dot{\boldsymbol{X}} = F(\boldsymbol{X}) = [F_1(\boldsymbol{X}), F_2(\boldsymbol{X}), \ldots, F_{3N}(\boldsymbol{X})]^T\,. \tag{21}$$

The corresponding Jacobian of Eq. (21) at an equilibrium point P_l can be written as

$$J_l = \left(\frac{\partial F_i(P_l)}{\partial x_j}\right)_{3N \times 3N}\,. \tag{22}$$

Denote $\sigma(A)$ as the spectrum of matrix A, and

$$M(A_l) = \max\{\mathrm{Re}\,[\lambda] : \lambda \in \sigma(A_l)\}\,,$$
$$M(J_l) = \max\{\mathrm{Re}\,[\lambda] : \lambda \in \sigma(J_l)\}\,. \tag{23}$$

Then for $b > 0$

$$M(A_0) > 0, \quad M(J_0) > 0, \quad \sigma(A_1) = \sigma(A_2)\,. \tag{24}$$

Table 1 Cell parameters and corresponding dynamic properties of the 3D Lorenz equations and CLCM CNN's, where $\sigma = 10$, $\mu = 3$, $k = 0.001$. Symbols $\Downarrow$, tnp, and $\oplus$ indicate that convergent patterns, twisting-n-period patterns, and chaotic patterns observed near to or far from the corresponding cell equilibrium points (CEDs) Q_1 and Q_2, respectively. Symbols 3D and HD stand for the 3D Lorenz equations and the CLCM CNN's, respectively. The numbers which are marked by a $*$ indicate that the corresponding cell parameters lie on the edge of chaos domain.

No.	b	r	CEDs Q_1 and Q_2	$M(A_1)$	$M(J_1)$	Patterns	
						3D	HD
1	0.04	45	$\pm 1.3266, \pm 1.3266, 44.0000$	0.0433	0.0419	$t1p$	$\oplus$
2	0.04	22	$\pm 0.9165, \pm 0.9165, 21.0000$	0.0108	0.0095	$t1p$	$\oplus$
3*	0.04	15	$\pm 0.7483, \pm 0.7483, 14.0000$	-0.0006	0.0007	$t1p \Downarrow$	$\oplus$
4*	0.04	10	$\pm 0.6000, \pm 0.6000, 9.0000$	-0.0067	-0.0079	$t1p \Downarrow$	$\Downarrow$
5*	0.04	7	$\pm 0.4899, \pm 0.4899, 6.0000$	-0.0111	-0.0123	$\Downarrow$	$\Downarrow$
6	0.25	45	$\pm 3.3166, \pm 3.3166, 44.0000$	0.2173	0.2151	$t1p$	$\oplus$
7	0.25	17	$\pm 2.0000, \pm 2.0000, 16.0000$	0.0152	0.0135	$t1p$	$\oplus$
8*	0.25	14	$\pm 1.8028, \pm 1.8028, 13.0000$	-0.0095	-0.0110	$t1p \Downarrow$	$\Downarrow$
9*	0.25	12	$\pm 1.6583, \pm 1.6583, 11.0000$	-0.0263	-0.0278	$t1p \Downarrow$	$\Downarrow$
10*	0.25	10.5	$\pm 1.5411, \pm 1.5411, 9.5000$	-0.0391	-0.0406	$\oplus \Downarrow$	$\Downarrow$
11*	0.25	10	$\pm 1.5000, \pm 1.5000, 9.0000$	-0.0434	-0.0449	$\Downarrow$	$\Downarrow$
12	0.55	45	$\pm 4.9193, \pm 4.9193, 44.0000$	0.3711	0.3684	$\oplus$	$\oplus$
13	0.55	35	$\pm 4.3243, \pm 4.3243, 34.0000$	0.2587	0.2561	$\oplus$	$\oplus$
14	0.55	32	$\pm 4.1292, \pm 4.1292, 31.0000$	0.2222	0.2197	$t4p$	$\oplus$
15	0.55	31	$\pm 4.0620, \pm 4.0620, 30.0000$	0.2097	0.2072	$t2p$	$\oplus$
16	0.55	17	$\pm 2.9665, \pm 2.9665, 16.0000$	0.0150	0.0130	$t2p$	$\oplus$
17*	0.55	15	$\pm 2.7749, \pm 2.7749, 14.0000$	-0.0164	-0.0184	$t2p \Downarrow$	$\Downarrow$
18*	0.55	11	$\pm 2.3452, \pm 2.3452, 10.0000$	-0.0829	-0.0847	$\Downarrow$	$\Downarrow$
19	0.60	45	$\pm 5.1381, \pm 5.1381, 44.0000$	0.3898	0.3870	$\oplus$	$\oplus$
20	0.60	25	$\pm 3.7947, \pm 3.7947, 24.0000$	0.1370	0.1346	$\oplus$	$\oplus$
21	0.60	17	$\pm 3.0984, \pm 3.0984, 16.0000$	0.0135	0.0113	$\oplus$	$\oplus$
22*	0.60	15	$\pm 2.8983, \pm 2.8983, 14.0000$	-0.0202	-0.0222	$\oplus \Downarrow$	$\Downarrow$
23*	0.60	11	$\pm 2.4495, \pm 2.4495, 10.0000$	-0.0915	-0.0934	$\Downarrow$	$\Downarrow$
24	1	45	$\pm 6.6332, \pm 6.6332, 44.0000$	0.4920	0.4888	$\oplus$	$\oplus$
25	1	19	$\pm 4.2426, \pm 4.2426, 18.0000$	0.0344	0.0317	$\oplus$	$\oplus$
26*	1	15	$\pm 3.7417, \pm 3.7417, 14.0000$	-0.0626	-0.0602	$\oplus \Downarrow$	$\Downarrow$
27	1	14	$\pm 3.6056, \pm 3.6056, 13.0000$	-0.0854	-0.1403	$\Downarrow$	$\Downarrow$
28	2	45	$\pm 9.3808, \pm 9.3808, 44.0000$	0.5357	0.5322	$\oplus$	$\oplus$
29	2	23	$\pm 6.6332, \pm 6.6332, 22.0000$	0.0463	0.0430	$\oplus$	$\oplus$
30	2	21.5	$\pm 6.4031, \pm 6.4031, 20.5000$	0.0022	-0.0011	$\oplus$	$\Downarrow$
31*	2	20	$\pm 6.1644, \pm 6.1644, 19.0000$	-0.0441	-0.0473	$\Downarrow$	$\Downarrow$

Using formulas (17) $\sim$ (24) and Theorems 1 $\sim$ 4, the locally passive domains, the locally active domains, and the edges of chaos with respect to Q_i's of a CLCM cellular neural network can be numerically calculated via computer programs. Now let, in Eqs (10) $\sim$ (12), the parameter $\sigma = 10$ fixed and the parameters b and r vary in the intervals [0, 2] and [0, 50], respectively. Our numerical calculation results are shown in Fig. 1. It can be concluded as follows:

- The bifurcation diagram with respect to the equilibrium point Q_0 has only a locally active unstable domain.
- The bifurcation diagrams with respect to the equilibrium points Q_1 and Q_2 [see Eq. (17)] are identity, and have not locally passive domains.

Now let us simulate numerically the 3-dimensional (3D) Lorenz equations and the CLCM cellular neural networks based on the bifurcation graph given in Fig. 1. The simulation results are shown in Table 1 and Figs 2 $\sim$ 6, respectively. Our numerical simulations show that

- The qualitative behaviors of the 3D Lorenz equations and the corresponding CLCM cellular neural network may be similar (see the parameter groups: Nos 5, 11 $\sim$ 13, 18 $\sim$ 21, 23 $\sim$ 25, 27 $\sim$ 29, and 31 listed in Table 1, Figs 5 and 6) or different (see the parameter groups: Nos 1 $\sim$ 4, 6 $\sim$ 10, 14 $\sim$ 17, 22, 26, and 30 listed in Table 1, Figs 2 $\sim$ 4) depending on the locations of selected cell parameters.
- The twisting-oscillation or the chaotic orbits of the 3D Lorenz equations can exist in the interior of the edge of the chaos (see the parameter groups: Nos 3, 4, 8 $\sim$ 10, 17, 22, and 26 and Fig. 3), in which the maximum real parts of the eigenvalues of the Jacobian matrices [Eq. (22)] are less than zero. This fact seems to imply that the edge of chaos may predict the emergency of the complex behaviors of the 3D Lorenz equations (furthermore general 3D nonlinear equations) far from their stable equilibrium points although it cannot assert exactly what kinds of complex behaviors can happen.
- The behaviors of the CLCM cellular neural network seem to be able to be determined successfully via the local activity principle. Roughly speaking, if the parameters group of the CLCM cellular neural networks are located in the active unstable region (see Fig. 1), the dynamics of the corresponding CLCM cellular neural networks always exhibit chaos (see the parameter groups: Nos 1 $\sim$ 3, 6, 7, 12 $\sim$ 16, 19 $\sim$ 21, 24, 25, 28, 29, and Figs 2 and 4 $\sim$ 6); otherwise are always convergent if the parameter groups are selected on the edge of chaos domain (see the parameter groups indicated by a $*$ given in Table 1 and Fig. 3).

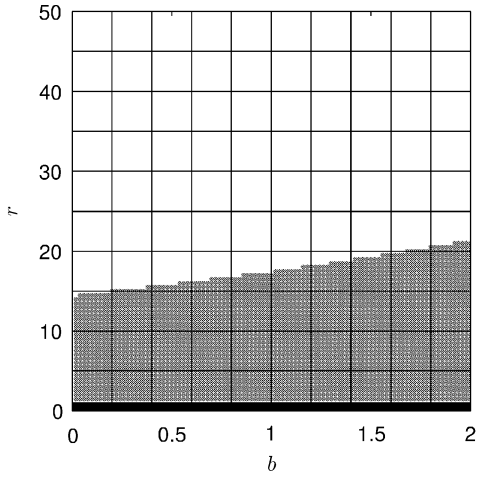

Fig. 1 Bifurcation diagram of the CLCM CNN with two ports at cross section $b \in [0,2]$, $r \in [0,50]$ with respect to the equilibrium point Q_1 or Q_2. The domains are coded as follows: edge of chaos (light black), locally active unstable domain (white). The domains coded with black stands for that no nonzero equilibrium point exists.

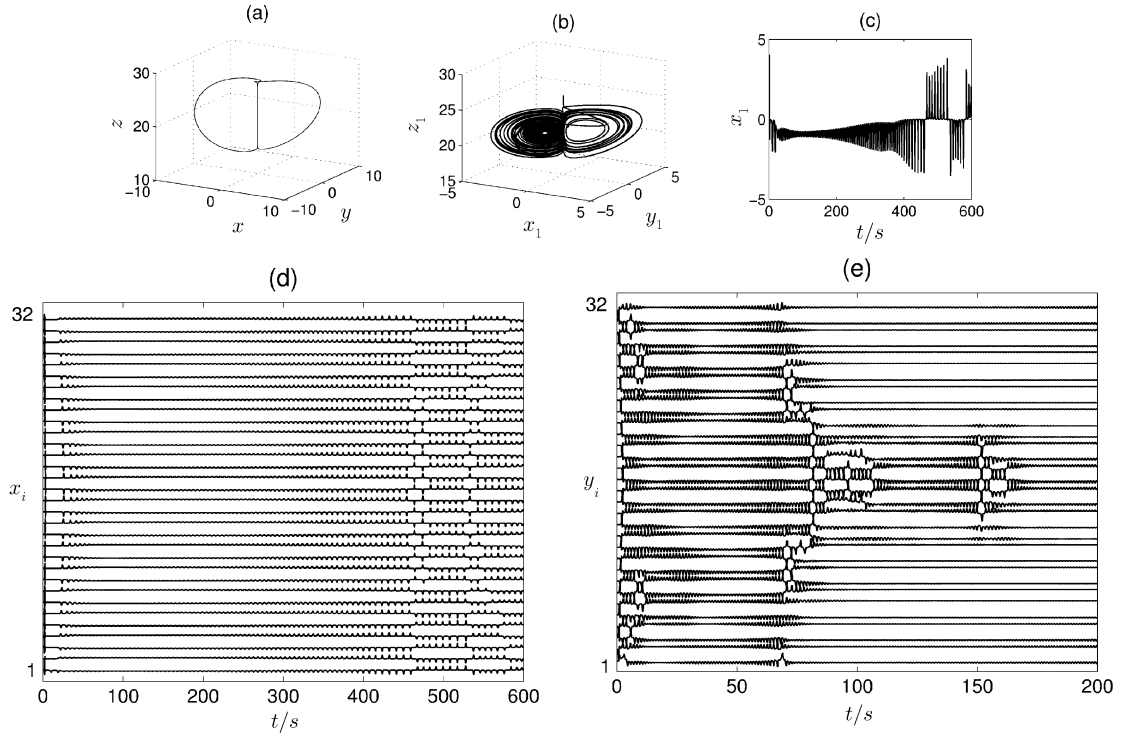

Fig. 2 Graphs generated by the parameter group No. 2 listed in Table 1. (a) The trajectory of the state variables x, y, and z of the Lorenz equations, initial conditions: $(x(0), y(0), z(0)) = (0.0005, -0.0005, 26.0921)$; (b) and (c) The chaotic trajectory and the time evolution of the state variables x_1, y_1, and z_1 of the CLCM CNN; (d) and (e) The graphs of the time evolution of the state variables x_i's, and y_i's of the CLCM CNN, initial conditions: $(x_1(0), y_1(0), z_1(0)) = (0.0005, -0.0005, 26.0921)$, and $(x_i(0), y_i(0), z_i(0)) = (0, 0, 0)$, $i = 2, 3, \ldots, 32$.

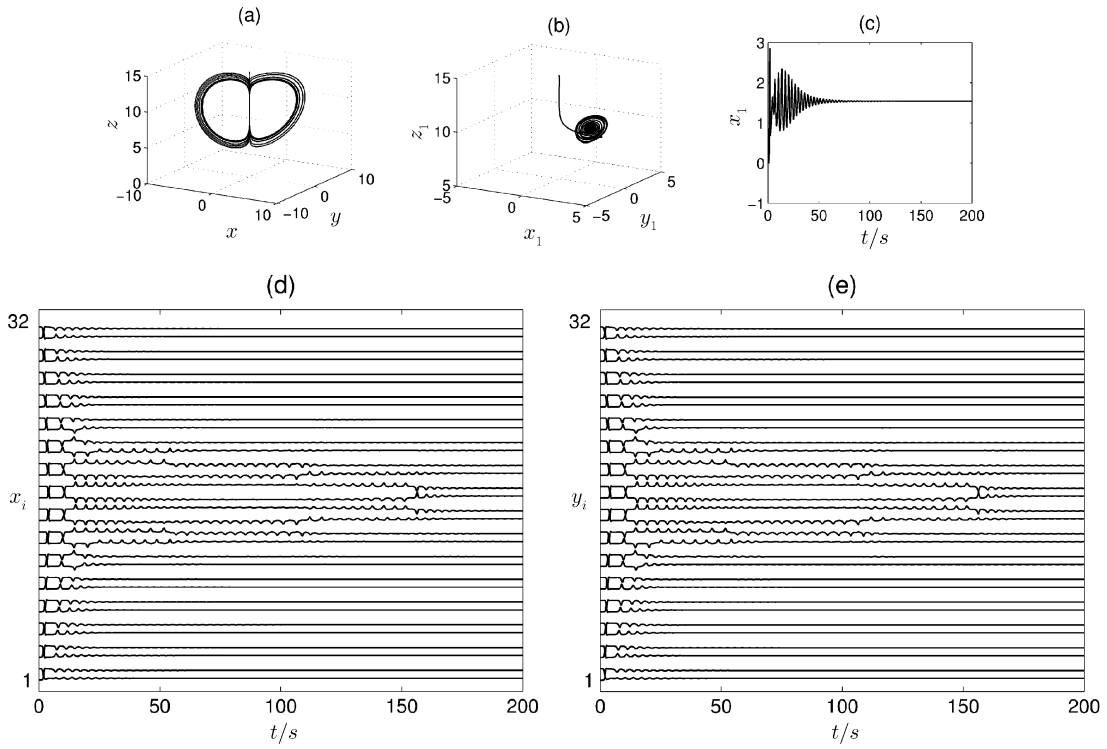

Fig. 3 Graphs generated by the parameter group No. 10 listed in Table 1. (a) The chaotic trajectory of the state variables x, y, and z of the Lorenz equations, initial conditions: $(x(0), y(0), z(0)) = (-0.0160, 0.0377, 14.6493)$; (b) and (c) The convergent trajectory and the time evolution of the state variables x_1, y_1, and z_1 of the CLCM CNN; (d) and (e) The graphs of the time evolution of the state variables x_i's and y_i's of the CLCM CNN, initial conditions: $(x_1(0), y_1(0), z_1(0)) = (-0.0160, 0.0377, 14.6493)$, and $(x_i(0), y_i(0), z_i(0)) = (0, 0, 0)$, $i = 2, 3, \ldots, 32$.

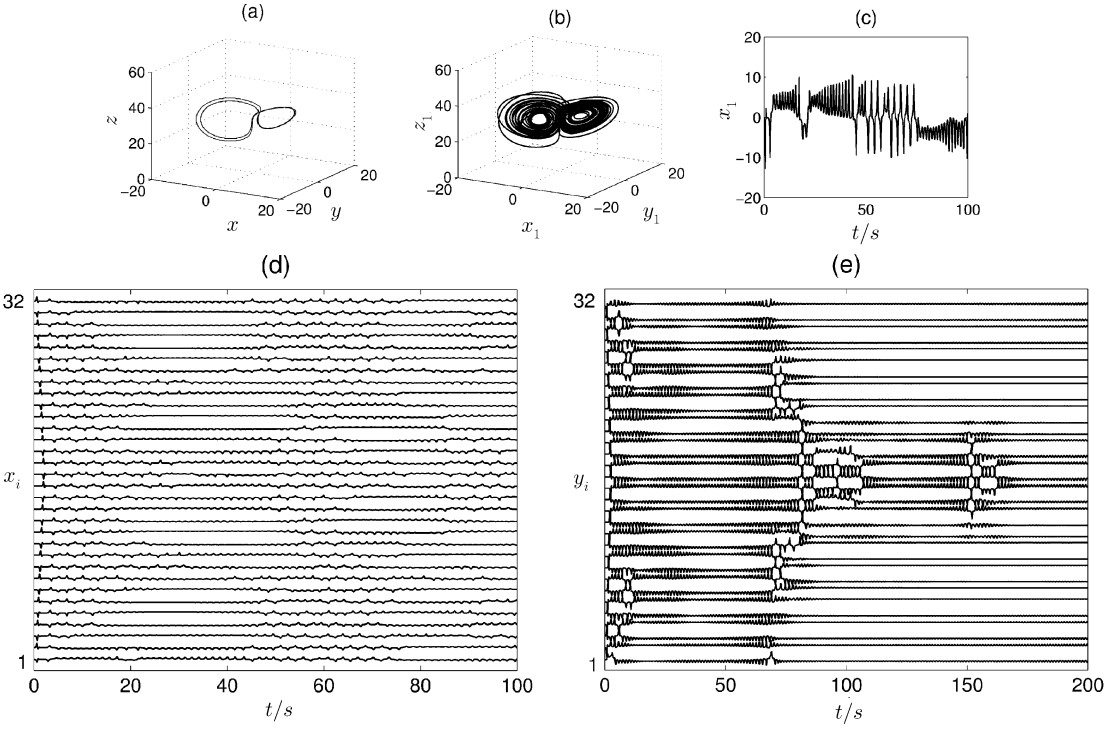

Fig. 4 Graphs generated by the parameter group No. 15 listed in Table 1. (a) The twisting-2-period trajectory of the state variables x, y, and z of the Lorenz equations, initial conditions: $(x(0), y(0), z(0)) = (-0.9400, -1.3855, 21.9583)$; (b) and (c) The chaotic trajectory and the time evolution of the state variables x_1, y_1, and z_1 of the CLCM CNN. (d) and (e) The graphs of the time evolution of the state variables x_i's and y_i's of the CLCM CNN, initial conditions: $(x_1(0), y_1(0), z_1(0)) = (-0.9400, -1.3855, 21.9583)$, and $(x_i(0), y_i(0), z_i(0)) = (0, 0, 0)$, $i = 2, 3, \ldots, 32$.

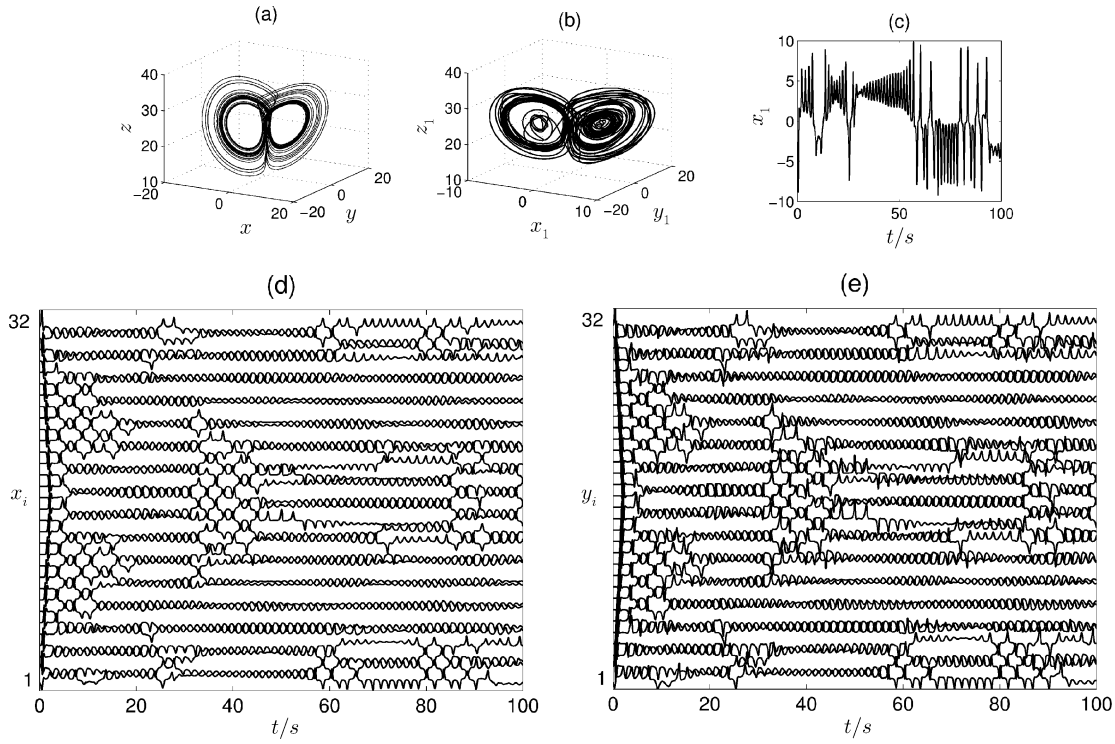

Fig. 5 Graphs generated by the parameter group No. 20 listed in Table 1. (a) The chaotic trajectory of the state variables x, y, and z of the Lorenz equations, initial conditions: $(x(0), y(0), z(0)) = (-2.6400, -4.3002, 17.9776)$; (b) and (c) The chaotic trajectory and the time evolution of the state variables x_1, y_1, and z_1 of the CLCM CNN; (d) and (e) The graphs of the time evolution of the state variables x_i's and y_i's of the CLCM CNN, initial conditions: $(x_1(0), y_1(0), z_1(0)) = (-2.6400, -4.3002, 17.9776)$ and $(x_i(0), y_i(0), z_i(0)) = (0, 0, 0)$, $i = 2, 3, \ldots, 32$.

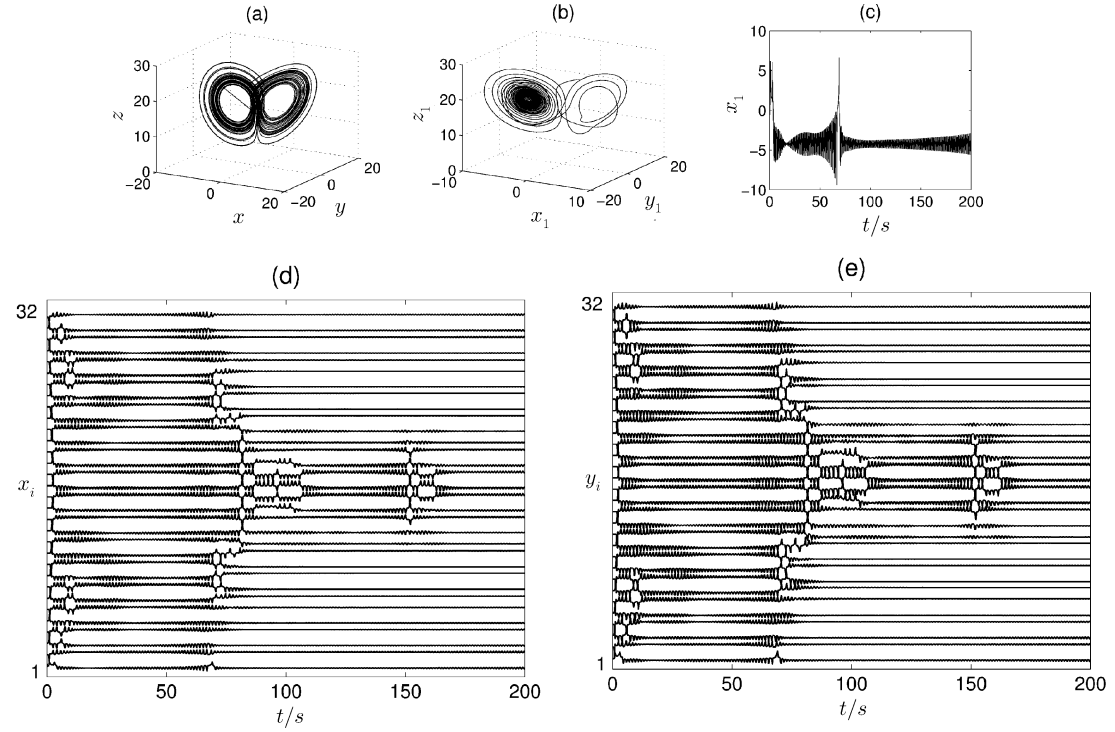

Fig. 6 Graphs generated by the parameter group No. 25 listed in Table 1. (a) The chaotic trajectory of the state variables x, y, and z of the Lorenz equations, initial conditions: $(x(0), y(0), z(0)) = (2.9, -1.3, 25)$; (b) and (c) The chaotic trajectory and the time evolution of the state variables x_1, y_1, and z_1 of the CLCM CNN; (d) and (e) The graphs of the time evolution of the state variables x_i's and y_i's of the CLCM CNN, initial conditions: $(x_1(0), y_1(0), z_1(0)) = (2.9, -1.3, 25)$ and $(x_i(0), y_i(0), z_i(0)) = (0, 0, 0)$, $i = 2, 3, \ldots, 32$.

4 Concluding Remarks

Coupled nonlinear dynamical systems (CND's) have been widely studied in recent years. However the dynamical properties of the CND's are difficult to be dealt with. The local activity criteria of CNN's provide a new tool to the research on the CND's cell models. This paper uses the criteria to study firstly the physical CND — the coupled Lorenz-cell model with one viscous coupling and one thermal coupling terms rather than the CNN's with reaction-diffusion terms dealt with previously.[10−15] It has also been found that for the parameters $\sigma = 10$, $\mu = 3$, $k = 0.001$, $b = 1$, and $N = 32$, the corresponding CLCM CNN and the standard Lorenz system can both exhibit chaos for r down to about 19 (see Fig. 6) rather than 23 announced in Ref. [18]; the dynamics of the CLCM and the standard Lorenz system may be quite different (see Table 1) rather than similar to the standard Lorenz system stated in Ref. [17].

Our numerical studies demonstrate that the edge of chaos appears to explain well the reason of the emergence of the complex orbits of the standard Lorenz system, and predict well the appearing of the chaotic patterns or divergent patterns of the CLCM CNN. The effectiveness of the local activity principle in the study for the emergence of complex patterns in a homogeneous lattice formed by coupled cells is once again confirmed.

Acknowledgment

One of the authors (MIN) would like to thank Prof. L.O. Chua for directing him to study the local activity theory.

Appendix

Lemma 2 If $Y_Q^H(s)$ is not a self-adjoint operator from $\mathbb{C}^n \longrightarrow \mathbb{C}^n$ then $Y_Q^H(s)$ is not a positive semi-definite matrix.

Proof It follows from Theorem 3.10-3 of Ref. [19].

Lemma 3 If $Y_Q^{H\dagger}(s) = Y_Q^H(s)$ and $Y_Q^H(s)$ is not a positive semi-definite matrix at some $\mathrm{i}\omega = \mathrm{i}\omega_0 \in \mathrm{i}\mathbb{R}$, if, and only if, there is at least one $\lambda < 0$ *s.t.* $\lambda \in \sigma(Y_Q^H(\mathrm{i}\omega))$.

Proof It is the conclusion of Theorem 9.2-1 of Ref. [19].

Proof of Theorem 1 By the definition of pole, formula (8) implies that Theorem 1 holds.

Proof of Theorem 2 Firstly, from Eq. (8) we obtain

$$Y_Q^H(\mathrm{i}\omega) = \begin{bmatrix} -2a_{11} + \dfrac{2a_{13}a_{31}a_{33}}{a_{33}^2+\omega^2} & -a_{12} - a_{21} + \dfrac{c + \mathrm{i}\omega d}{a_{33}^2+\omega^2} \\ -a_{12} - a_{21} + \dfrac{c - \mathrm{i}\omega d}{a_{33}^2+\omega^2} & -2a_{22} + \dfrac{2a_{23}a_{32}a_{33}}{a_{33}^2+\omega^2} \end{bmatrix}. \tag{A1}$$

Therefore, we conclude that $Y_Q^H(s)$ is a self-adjoint operator. In this case, the eigenvalue λ of matirx $Y_Q^H(\mathrm{i}\omega)$ satisfies the following equation

$$|\lambda I - Y_Q^H(\mathrm{i}\omega)| = \lambda^2 + a_1\lambda + a_0 = 0\,, \tag{A2}$$

where

$$a_1 = 2(a_{11} + a_{22}) - \frac{2(a_{13}a_{31}a_{33} + a_{23}a_{32}a_{33})}{a_{33}^2+\omega^2}\,, \tag{A3}$$

$$a_0 = 4\Big(a_{11} - \frac{b}{a_{33}^2+\omega^2}\Big)\Big(a_{22} - \frac{e}{a_{33}^2+\omega^2}\Big) - \Big(a_{12} + a_{21} - \frac{c}{a_{33}^2+\omega^2}\Big)^2 - \frac{\omega^2 d^2}{(a_{33}^2+\omega^2)^2}\,, \tag{A4}$$

where $b = a_{13}a_{31}a_{33}$, $e = a_{23}a_{32}a_{33}$, $c = a_{13}a_{32}a_{33} + a_{23}a_{31}a_{33}$, $d = a_{13}a_{32} - a_{23}a_{31}$. Consequently, it follows, from Lemmas 2 and 3, that $Y_Q^H(\mathrm{i}\omega)$ is not a positive semi-definite matrix at some $\omega = \omega_0$, if, and only if

$$a_1 > 0 \quad \text{or} \quad a_0 < 0\,. \tag{A5}$$

Case 1 Testing condition $a_1 > 0$

(i) If $a_{11} + a_{22} > 0$, then it follows from Eq. (A3) that if ω is large enough, $a_1 > 0$. Hence condition 1 implies that $Y_Q^H(\mathrm{i}\omega)$ satisfies condition (ii) in Lemma 1.

(ii) If $a_{11} + a_{22} \le 0$ and $a_{33}(a_{13}a_{31} + a_{23}a_{32}) \ge 0$, then $a_1 > 0$ cannot hold for any $\omega \in \mathbb{R}$.

(iii) If $a_{11} + a_{22} \le 0$ and $a_{33}(a_{13}a_{31} + a_{23}a_{32}) < 0$, then $a_1 > 0$ has a solution $\omega \in \mathbb{R} \Longleftrightarrow a_{11} + a_{22} - (a_{13}a_{31} + a_{23}a_{32})/a_{33} > 0$. Therefore condition 2 guarantees that condition (ii) in Lemma 1 holds.

Case 2 Testing condition $a_0 < 0$

(a) If $4a_{11}a_{22} - (a_{12} - a_{21})^2 < 0$, then it follows from Eq. (A4) that if ω is large enough, $a_0 < 0$. That is, if condition *3* holds then condition (ii) in Lemma 1 is satisfied.

(b) If $4a_{11}a_{22} - (a_{12} - a_{21})^2 \ge 0$, let $L(\omega^2) = a_0$.

a) If $L(0) \geq 0$, since $\lim_{\omega\to\infty} L(\omega^2) = 0$, we only need to examine the minimum of $L(\omega^2)$ in $[0, +\infty]$. Solving $\dot{L}_{\omega^2}(\omega^2) = 0$, we obtain

$$4(ba_{22} + ea_{11})(a_{33}^2 + \omega^2) - 8be - 2c(a_{12} + a_{21})(a_{33}^2 + \omega^2) + 2c^2 - d^2(a_{33}^2 + \omega^2) + 2\omega^2 d^2 = 0\,,$$

$$\omega^{*2} = \frac{2a_{33}^2 d^2 + 8be - 2c^2}{4(ba_{22} + ea_{11}) - 2c(a_{12} + a_{21}) + d^2} - a_{33}^2\,.$$

It follows that condition *4* implies that $Y_Q^H(\mathrm{i}\omega)$ satisfies condition (ii) in Lemma 1.

b) If $a_{33} \neq 0$ then condition *5* holds to guarantee $L(0) < 0$. Otherwise if $a_{33} = 0$ then condition *6* implies that $L(0) < 0$. Consequently in both cases condition (ii) in Lemma 1 is satisfied.

To sum up, we complete the proof.

Proof of Theorem 3 $Y_Q(s)$ has a simple pole $s = \mathrm{i}\omega$ on the imaginary axis $\Longleftrightarrow$ $a_{33} = 0$ and $\max\{|a_{13}a_{31}|, |a_{13}a_{32}|, |a_{23}a_{31}|, |a_{23}a_{32}|\} \neq 0$. In this case,

$$k_1 = \lim_{s\to 0} sY_Q(s) = \begin{bmatrix} -a_{13}a_{31} & -a_{13}a_{32} \\ -a_{23}a_{31} & -a_{23}a_{32} \end{bmatrix}.$$

Therefore if $a_{13}a_{32} \neq a_{23}a_{31}$, then $Y_Q(s)$ satisfies condition (iii) in Lemma 1. On the other hand, if $a_{13}a_{32} = a_{23}a_{31}$, then $Y_Q(s)$ is a Hermitian matrix. Since

$$\det|\lambda I - k_1| = \lambda^2 + \lambda(a_{13}a_{31} + a_{23}a_{32}) + a_{13}a_{31}a_{23}a_{31} - a_{13}^2 a_{32}^2\,.$$

Consequently, if $a_{13}a_{31} + a_{23}a_{32} > 0$ or $a_{13}a_{31}a_{23}a_{31} - a_{13}^2 a_{32}^2 < 0$, then $Y_Q(s)$ satisfies condition (iii) in Lemma 1.

Finally, $Y_Q(s)$ has a simple $\mathrm{i}\omega$-axis pole at infinity and

$$\lim_{\omega_p\to\infty} \frac{Y_Q(\mathrm{i}\omega_p)}{\mathrm{i}\omega_p} = I$$

is a positive-definite matrix.

This completes the proof.

Proof of Theorem 4 Equation (8) shows that $Y_Q(s)$ has no multiple pole on the imaginary axis.

References

[1] J.H. Holland, *Emergence: From Chaos to Order*, Addision-Wesley, Reading MA (1998).

[2] H. Haken, Int. J. Bifurcation and Chaos **7** (1997) 1927.

[3] *Artificial Life: An Overview*, ed. G.G. Langton, MS: MIT Press, Cambridge (1995).

[4] M. Gell-Mann, *The Quark and the Jaguar: Adventures in the Simple and the Complex*, Freeman, New York (1994).

[5] M.M. Waldrop, *Complexity: The Emerging Science at the Edge of Order and Chaos*, Simon & Schuster, New York (1992).

[6] G. Nicolis and I. Prigogine, *Exploring Complexity: An Introduction*, Freeman, New York (1989).

[7] L.O. Chua and L. Yang, IEEE Trans. Circuits Syst. **35** (1988) 1257, 1273.

[8] L.O. Chua, Int. J. Bifurcation and Chaos **7** (1997) 2219.

[9] L.O. Chua, IEEE Trans. Circuits Syst. I: Fundamental Theory and Applications **46** (1999) 71.

[10] R. Dogaru and L.O. Chua, Int. J. Bifurcation and Chaos **8** (1998) 211.

[11] R. Dogaru and L.O. Chua, Int. J. Bifurcation and Chaos **8** (1998) 1107.

[12] R. Dogaru and L.O. Chua, Int. J. Bifurcation and Chaos **8** (1998) 2321.

[13] L. Min, K.R. Crounse, and L.O. Chua, Int. J. Bifurcation and Chaos **10** (2000) 25.

[14] L. Min, K.R. Crounse, and L.O. Chua, Int. J. Bifurcation and Chaos **10** (2000) 1295.

[15] L. Min and N. Yu, J. Univ. Sci. Tech. Beijing **7** (2000) 305.

[16] B.D.C. Anderson and S. Vongpanitlerd, *Network Analysis and Synthesis: A Modern Systems Theory Approach*, Printice-Hall Electrical Engineering Series, Prentice-Hall Network Series, Englewood Cliffs, NJ: Prentice-Hall (1973).

[17] E.A. Jackson and A. Kodogeorgiou, Phys. Lett. **A168** (1992) 270.

[18] K.A. Mirus and J.C. Sprott, Phys. Lett. **A256** (1999) 275.

[19] E. Kreyszig, *Introduction Functional Analysis with Applications*, John Wiley & Sons, New York (1978).